Supporting Information

Yan et al. 10.1073/pnas.0910811106

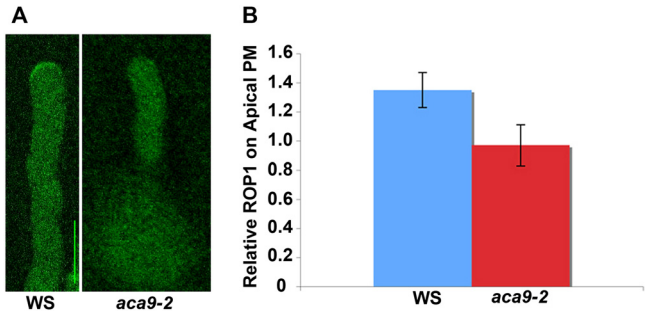

Fig. S1. Localization of ROP1 protein in *aca9–2* mutant pollen tubes. (*A*) Anti-ROP1 staining of a control WS wild-type pollen tube and an *aca9–2* pollen tube. (Scale bar: 10 μm.) (B) Quantitative analysis of the PM-localized ROP protein in WS and *aca9–2* pollen tubes ($n = 15$; $P < .05$, Student *t*-test). Error bars indicate SD. The relative ROP1 amount on apical PM is defined as the ratio of the mean value of the FITC signal localized to the apical PM and that localized to the cytosol. The mean intensity of FITC signals on the apical PM and in the cytosol was measured using MetaMorph 4.5 (Universal Imaging) for each median scan of immunostained pollen tubes. The mean intensity of the cytosolic part was obtained from an area 15 μm in circumference in the middle of the pollen tube, 2 μm away from the tips of the tubes.

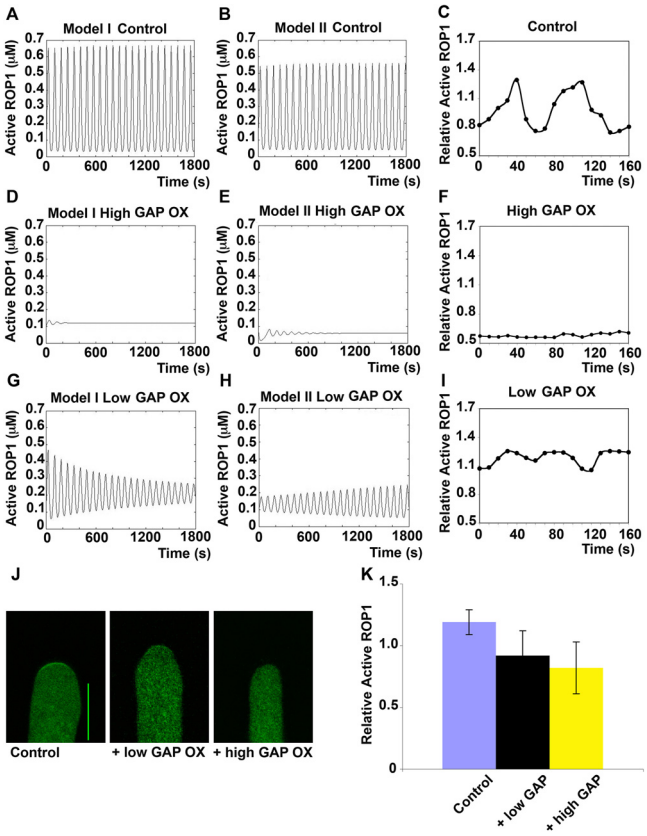

Fig. S2. Simulation and experimental validation of ROP1 activity oscillation in pollen tubes overexpressing RhoGAP. (*A* and *B*) Simulation of ROP1 activity oscillation in control pollen tubes using model I (*A*) and model II (*B*). (*C*) Experimental measurement of ROP1 activity oscillation in control pollen tubes. Relative ROP1 activity was measured as described in Fig. 3. Shown is a typical oscillating pollen tube with an amplitude of 0.5 (from 0.8 to 1.3) and a period of ≈80 s. Six out of 10 pollen tubes showed a similar oscillation pattern. (*D* and *E*) Simulations from model I (*D*) and model II (*E*) predicted that the apical ROP1 activity would be reduced to a low level and be nonoscillating in pollen tubes overexpressing RhoGAP. For model I, $\alpha_x = 0.35\ s^{-1}$. For model II, $\alpha_x = 2\ s^{-1}$. (*F*) Time-course analysis of ROP1 activity oscillation in a pollen tube with high RhoGAP overexpression. Here 0.1 μg of RopGAP1 plasmid was used for transformation, and relative ROP1 activity was determined as described in Fig. 3. Relative ROP1 activity was reduced to a basal level (< 0.8) and did not oscillate. All 30 pollen tubes examined showed a similar pattern. (*G* and *H*) Simulation from model I (*G*) predicted that a low level of RhoGAP overexpression would suppress the oscillation of apical ROP1 activity and make it very unstable. Simulation from model II (*H*) predicted that ROP1 activity would still oscillate, but with much smaller amplitude, at a very low level of RhoGAP overexpression. For model I, $\alpha_x = 0.275\ s^{-1}$. For model II, $\alpha_x = 1.2\ s^{-1}$. (*I*) Time-course analysis of ROP1 activity oscillation in a pollen tube with a low level of RopGAP1 overexpression. Here 0.02 μg RopGAP1 plasmid was used for transformation, and relative ROP1 activity was determined as described in Fig. 3. Relative ROP1 activity was reduced to a low level and exibited fluctuations (1.1–1.2). Three out of 20 pollen tubes examined showed a similar pattern. Because of the low level of ROP1 activity, determining whether the fluctuating ROP1 activity reflects unstable oscillation or measurement variation is difficult. (*J*) Representative snapshot images of GFP-RIC4ΔC localization in control tubes and pollen tubes overexpressing low and high levels of RopGAP1. Each figure is the representative from 20 pollen tubes. (Scale bar: 10 μm.) (*K*) Quantitative analysis of GFP-RIC4ΔC distribution to the apical PM. Shown is the mean relative ROP1 activity in control tubes and pollen tubes with low and high levels of RhoGAP overexpression ($n = 20$; $P < .05$, Student *t*-test). Error bars indicate SD.

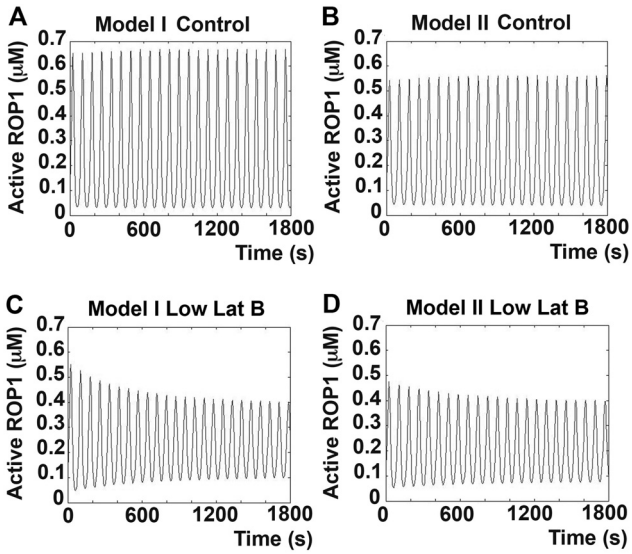

Fig. S3. Model simulation of ROP1 activity oscillation in pollen tubes, in which F-actin level is reduced by latrunculin B treatment. (*A* and *B*) Simulation of ROP1 activity oscillation in control pollen tubes using model I (*A*) and model II (*B*). (*C* and *D*) Simulations based on model I (*C*) and model II (*D*) predicted that the period of ROP1 activity oscillation would be unaffected, but its amplitude would be reduced in pollen tubes treated with low-level latrunculin B (0.5 nM). This prediction is consistent with the experimental data that we reported previously (1). For model I, $k = 4.8$. For model II, $k = 2.1$.

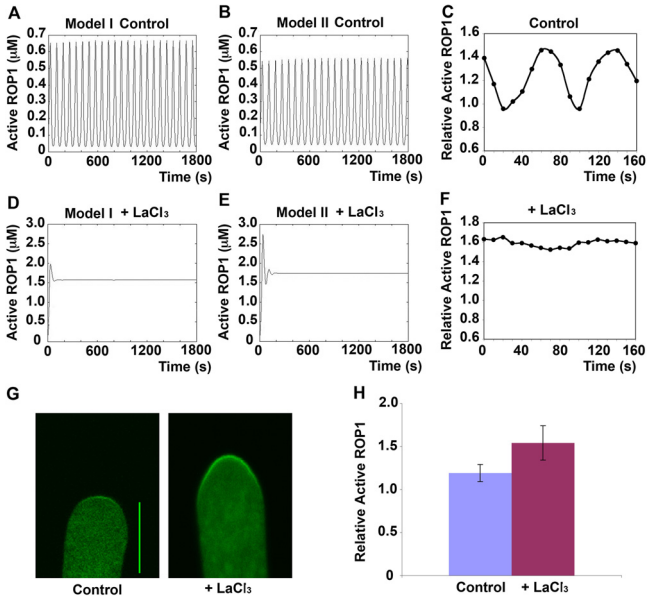

Fig. S4. Model simulation and experimental validation of ROP1 activity oscillation in pollen tubes with reduced calcium accumulation. (*A* and *B*) Simulation of ROP1 activity oscillation in control pollen tubes using model I (*A*) and model II (*B*). (*C*) Experimental measurement of ROP1 activity oscillation in control pollen tubes. Relative ROP1 activity was measured as described in Fig. 3. Shown is a typical oscillating pollen tube with an amplitude of 0.5 (from 0.95 to 1.45) and a period of ≈80 s. Six out of 10 pollen tubes showed a similar oscillation pattern. (*D* and *E*) Simulation of ROP1 activity oscillation in pollen tubes with diminished calcium accumulation. For model I, $\beta_y = 0.025\ s^{-1}$. For model II, $\beta_y = 0.025\ s^{-1}$. (*F*) Time-course analysis of relative ROP1 activity in a pollen tube treated with 10 μM $LaCl_3$. Relative ROP1 activity was constantly high (> 1.5) and lacked oscillation. All of the 20 pollen tubes examined showed a similar pattern. (*G*) GFP-RIC4ΔC localization in control and $LaCl_3$-treated pollen tubes. (Scale bar: 10 μm.) (*H*) Quantitative analysis of relative ROP1 activity in control and $LaCl_3$-treated pollen tubes ($n = 20$; $P < .05$, Student *t*-test). Error bars indicate SD.